

Cross-linking Chemistry of Squid Beak*[‡]

Received for publication, July 4, 2010, and in revised form, August 28, 2010. Published, JBC Papers in Press, September 24, 2010, DOI 10.1074/jbc.M110.161174

Ali Miserez^{‡1}, Daniel Rubin^{‡§2}, and J. Herbert Waite^{‡§¶1}

From the [‡]Marine Science Institute, the [§]Department of Molecular, Cell, and Development Biology, and the [¶]Department of Chemistry and Biochemistry, the University of California, Santa Barbara, California 93106

In stark contrast to most aggressive predators, *Dosidicus gigas* (jumbo squids) do not use minerals in their powerful mouthparts known as beaks. Their beaks instead consist of a highly sclerotized chitinous composite with incremental hydration from the tip to the base. We previously reported L-3,4-dihydroxyphenylalanine (dopa)-histidine (dopa-His) as an important covalent cross-link providing mechanical strengthening to the beak material. Here, we present a more complete characterization of the sclerotization chemistry and describe additional cross-links from *D. gigas* beak. All cross-links presented in this report share common building blocks, a family of di-, tri-, and tetra-histidine-catecholic adducts, that were separated by affinity chromatography and high performance liquid chromatography (HPLC) and identified by tandem mass spectroscopy and proton nuclear magnetic resonance (¹H NMR). The data provide additional insights into the unusually high cross-link density found in mature beaks. Furthermore, we propose both a low molecular weight catechol, and peptidyl-dopa, to be sclerotization agents of squid beak. This appears to represent a new strategy for forming hard tissue in animals. The interplay between covalent cross-linking and dehydration on the graded properties of the beaks is discussed.

Cephalopods such as squids, cuttlefish, and octopods are equipped with a hard beak that is as sharp as a knife and crucial for disabling prey and feeding. Beak chemistry has attracted much recent attention in materials science: in contrast to mammalian hard tissues, the beak is devoid of minerals, consisting instead of a composite of proteins and chitin fibers with varying degrees of hydration along the beak structure. In animals, this is a unique material design for hard tissues that function in biting. The *Dosidicus* beak biocomposite possesses a stiffness (elastic modulus, *E*) of 5 GPa at the distal tip that decreases incrementally to 50 MPa (wet conditions) in the proximal wing, which is tightly embedded within the muscular buccal mass (1). As the beak lacks any of the known strengthening entities previously associated with wear-resistant tissues such as biomineralization (2–5), metal ion cross-linking (6, 7), or protein halogenation (8, 9), it begs a question, namely, what sort of molecular

processing can impart such impressive physical properties? A deeper understanding of the mechanisms by which beaks are sclerotized is also likely to reveal novel chemical paradigms for the fabrication of robust and biocompatible composites for a variety of restorative applications. Furthermore, synthesis of such polymer-based composite materials could inspire environmentally friendly routes as *Dosidicus* beak is formed under ambient seawater conditions and is wholly nontoxic.

From a biochemical perspective the biomaterial most similar to *Dosidicus* beak is hard insect cuticle. Both are predominantly composed of chitin fibers, protein, and polyphenolic compounds (10, 11). In insect cuticle, the contribution of dehydration and cross-linking to sclerotization is notably controversial (12–15). α -Chitin fibers, because of their hydrophilic nature, are highly hydrated. Hence, the common view that protein cross-linking itself is the major mechanism leading to hardening and stiffening (12, 16–19) has been criticized by arguing that chitin dehydration via impregnation of hydrophobic proteins might instead be the main stiffening mechanism (13, 14). Most probably, the formation of a dense cross-linked network and dehydrated composite both contribute to hardening (15) and, therefore, a detailed identification of cross-links formed during beak maturation is essential. In both scenarios, chemical bonds play a crucial role in the beak mechanics by increasing the load carried by the proteins or by providing an efficient hydrophobic “coating” around chitin nanofibers, thus preventing softening of the latter by water adsorption.

One beak-derived cross-link previously identified by tandem mass spectroscopy (MS/MS)³ was a dimer of L-3,4-dihydroxyphenylalanine (dopa)-histidine (dopa-His) (20), but the specific linkage between the imidazole and the catechol ring could not be assigned. In this report, a more complete characterization of the sclerotization chemistry and description of additional cross-links from *Dosidicus gigas* beak are presented. All of the cross-links in this report share common building blocks, which were identified by MS/MS and proton nuclear magnetic resonance (¹H NMR). We propose both a low molecular weight catechol, and peptidyl-dopa, to be sclerotization agents of squid beak and suggest a mechanism by which the hard beak tissue is formed.

MATERIALS AND METHODS

***Dosidicus* Beak Samples**—*D. gigas* beaks (including the surrounding buccal mass) were dissected from animals collected off the coast of Ventura, California, in June 2007 and stored at –80 °C until needed. Beaks were separated from their buccal

* This work was supported, in whole or in part, by National Institutes of Health Grant R01DE018468. This work was also supported by a Nanyang Technological University start-up grant (to A. M.).

[‡] The on-line version of this article (available at <http://www.jbc.org>) contains Fig. S1.

¹ To whom correspondence should be sent at the present address: School of Materials Science and Engineering, Nanyang Technological University, Singapore, 639798. Tel.: 65-6316-8979; Fax: 65-6790-9081; E-mail: ali.miserez@ntu.edu.sg.

² Present address: School of Engineering and Applied Sciences, Harvard University, Cambridge, MA 02138.

³ The abbreviations used are: MS/MS, tandem mass spectrometry; dopa, L-3,4-dihydroxyphenylalanine; ESI, electrospray ionization; 4MC, 4-methylcatechol; Pa, pascal; TOF, time of flight.

Cross-linking Chemistry of Squid Beak

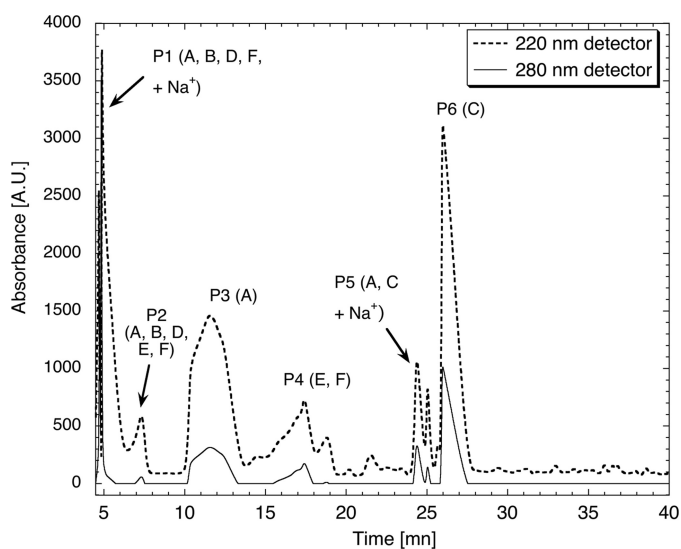
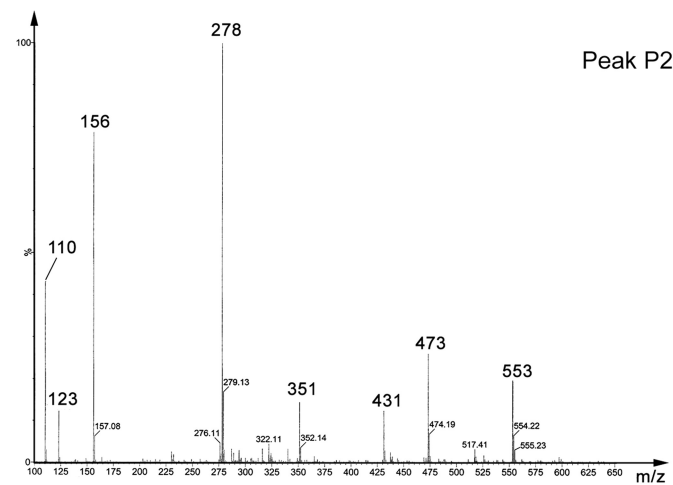


FIGURE 1. Reverse-phase HPLC elution profile of hydrolyzed beaks after phenylboronate affinity chromatography. Capital letters refer to catecholic compounds as identified by MS/MS and proton NMR. Two peaks (P3 and P6) consist of pure catecholic cross-links; the others are mixtures of cross-links.

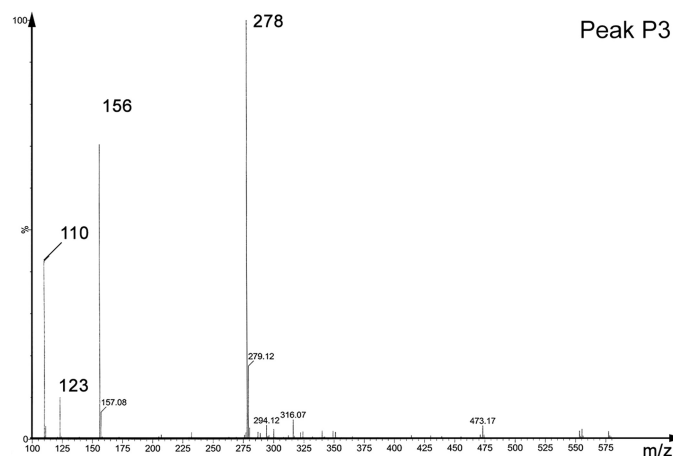
tissue (and the latter stored). The tanned regions were cut from the soft, untanned regions, and ground into a fine powder with mortar and pestle under liquid nitrogen.

Cross-link Isolation: Affinity Chromatography and HPLC—Beak was triturated by a mortar and pestle, and the powder was hydrolyzed *in vacuo* in 1-ml hydrolysis tubes using a standard hydrolysis solution consisting of 6 M HCl and 5% phenol. Hydrolysis was conducted at 110 °C for 24 h, after which the hydrolysates were flash-evaporated and washed thoroughly in Milli Q-water and methanol. Washed samples were then resuspended in 100 mM sodium phosphate (pH 7.5) buffer and centrifuged at 14,000 × g, and the soluble supernatant was passed through a phenylboronate affinity column (Affi-Gel boronate; Bio-Rad). Phenylboronate affinity chromatography captures *cis*-diols (e.g. catecholic compounds) by a pH-dependent complexation to boronate groups in the resin (21). This technique has previously been utilized for separation and analysis of catecholic compounds in other extracellular tissues or marine adhesives (22, 23). After loading the supernatant, the column was desalted with 2.5 mM NH_4HCO_3 and Milli-Q water, and the bound ligands were eventually released by eluting with ~3 column volumes of 5% acetic acid. Ligands captured were lyophilized and stored at -20 °C prior to subsequent separation. Confirmation of catecholic-based compounds was initially done using the Arnow colorimetric assay, in which mono- or unsubstituted catechols turn a pink to red color (24, 25).

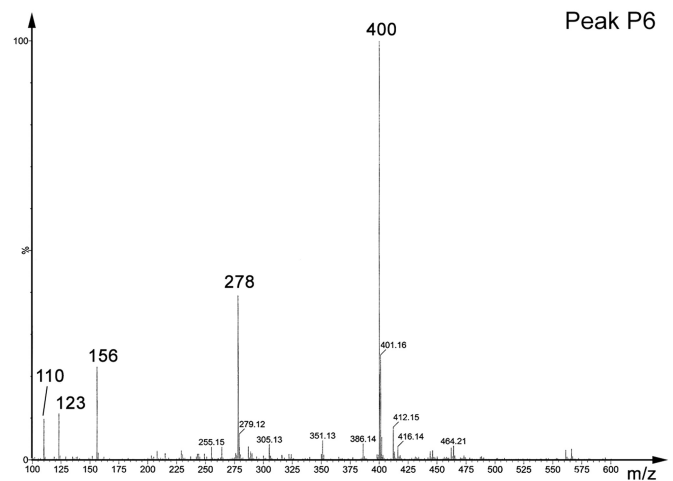
Preliminary mass spectrometric analyses (see “Tandem Mass Spectrometry”) detected multiple catecholic ligands after phenyl affinity chromatography. These were further isolated by High Performance Liquid Chromatography (HPLC) using a Varian Galaxie (Varian, Palo Alto, CA) system equipped with a dual wavelength diode array UV-visible detector set at 220 nm and 280 nm, the first for the polypeptide backbone and the second for detection of catecholic compounds. The lyophilized powder was resuspended in 5% acetic acid and applied to a Brownlee OD-300 C18 column (PerkinElmer Life Sciences). A



(a)



(b)

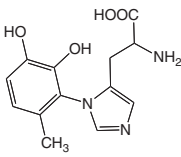
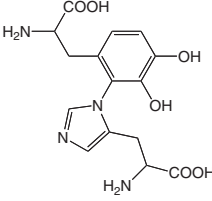
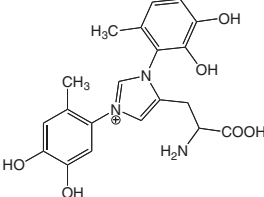
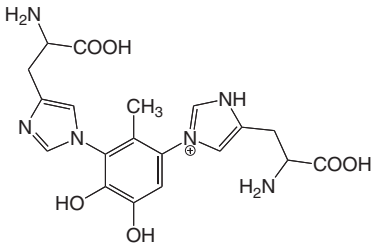
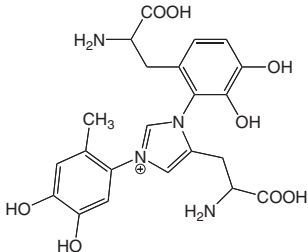
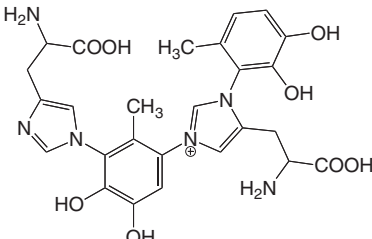


(c)

water/acetonitrile (with 1% trifluoroacetic acid) linear gradient system was employed with the following gradient steps: (i) 100% water for 5 min; (ii) 100 to 90% water in 40 min; (iii) 90 to

TABLE 1**Cross-link as identified by MS/MS**

The letters in the first column correspond to the letters in Fig. 1 (HPLC chromatogram).

Cross-link	<i>m/z</i>	Chemical structure	Name
A	278		4MC – His
B	351		Dopa – His
C	400		4MC – His – 4MC
D	431		His – 4MC – His
E	473		4MC – His – Dopa
F	553		His – 4MC – His – 4MC

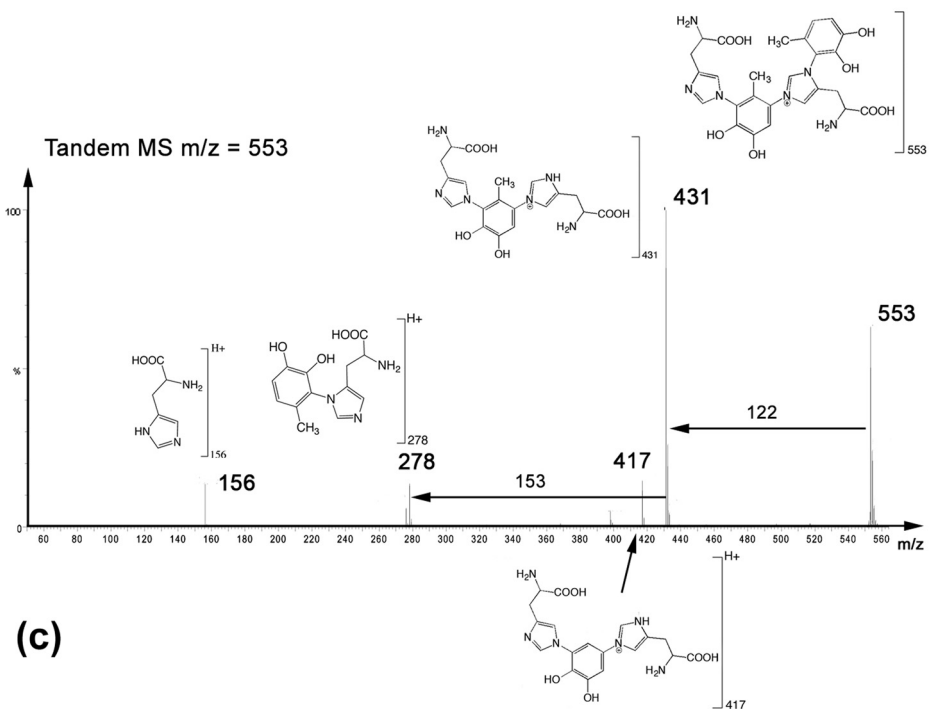
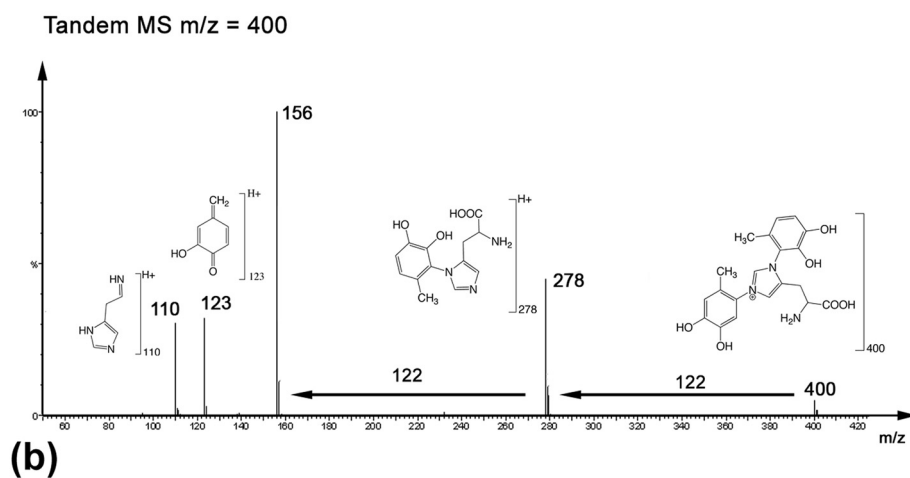
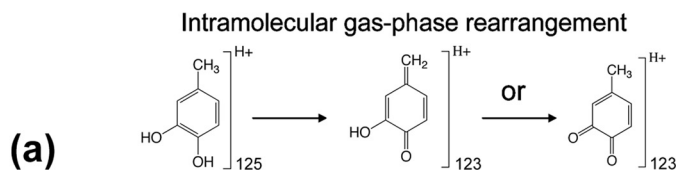
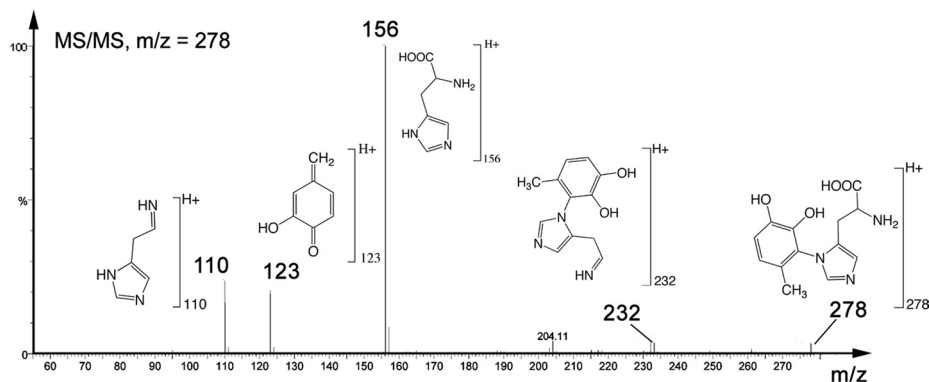
Cross-linking Chemistry of Squid Beak

0% water in 5 min; (iv) 0% water for 5 min (column cleaning). It was particularly critical to keep a shallow gradient in step (ii) to ensure adequate separation of the catecholic compounds. The collected fractions were lyophilized and redissolved in a 50:50 water/acetonitrile solution with 0.3 vol % formic acid for mass spectrometry analyses. Once purity of the fractions was verified, the remaining solution after affinity chromatography was separated into three additional HPLC runs. The fractions of interest were pooled, lyophilized, and resuspended in deuterium H_2O for 1H NMR analyses.

MS/MS—Peaks detected in HPLC spectra were analyzed by electrospray ionization (ESI) MS/MS using an Micromass QTOF2 quadrupole/time-of-flight mass spectrometer (Waters Corp., Milford, MA). Samples were injected into the electrospray source through a fused silica tubing attached to a syringe pump that continuously injected the sample at a rate of $5 \mu l/min$. Typical settings were a capillary tension of 3.5 kV, a cone tension of 45 V, and a collision voltage of 10 V for the MS mode. Once cross-links of interest were detected, they were subsequently fragmented at collision voltages of 20 and 35 V to obtain large or small molecular weight fragments, respectively. Fragmentation patterns were processed with the MassLynx software package and later manually analyzed for final cross-link determination.

Proton NMR—Isolated cross-links as well as pure histidine (Sigma) were resuspended in D_2O , and solution phase 1H NMR was recorded on a Bruker AVANCE 500-MHz spectrometer (Bruker, Fremont, CA) with tetramethylsilane as an external standard. Data acquisition time was dependent on sample concentration.

Isolation of Cross-link Precursor—Thin sections were carefully cut from partially frozen buccal masses. Buccal mass slices were then assayed using Arnow stain. Two small Arnow reactive glands were



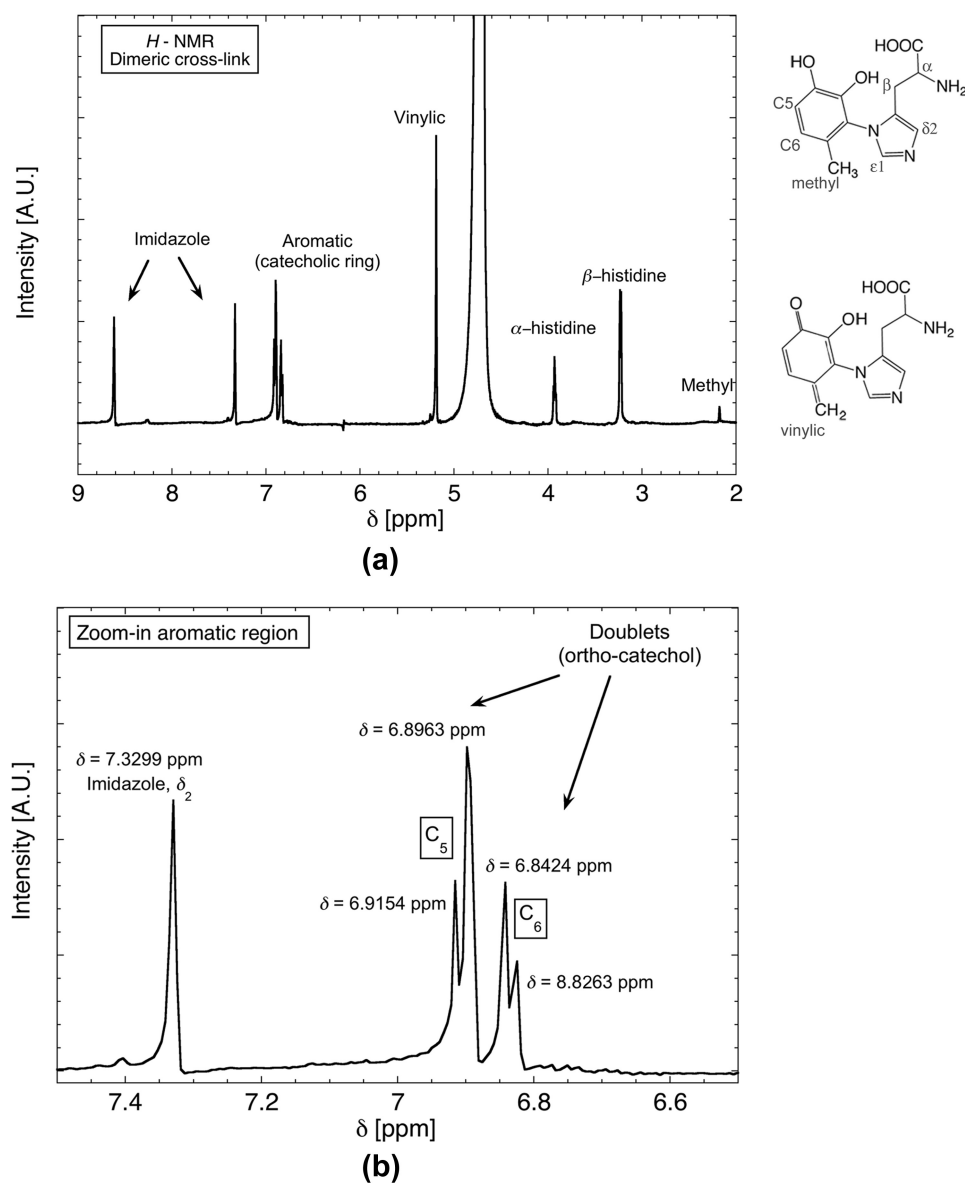


FIGURE 4. ^1H NMR spectra of the dimeric cross-link His-4MC ($m/z = 278$). *a*, both vinylic hydrogen and methyl peaks are detected, consistent with the co-existence of methylcatechol and quinone-methide. *b*, close-up view of the aromatic region, showing coupling of protons in the catecholic ring, consistent with an ortho arrangement of hydroxyls on the ring.

dissected and extracted in a 15-ml Kontes (Vineland, NJ) tissue grinder with 80% ethanol in water at 4 °C. Homogenates were centrifuged at $15,000 \times g$ for 30 min at 4 °C to pellet. The pellet was then reextracted in 0.5 M HCl, and the supernatant was separated using a size-exclusion column (Shodex KW 803) on a Gilson (Middleton, WI) HPLC system, using 5% acetic acid as the mobile phase. A peak with significant 280 nm absorbance was collected and assayed with the Arnow stain.

RESULTS

HPLC—Following capture by phenylboronate affinity chromatography, catecholic compounds were identified by their

Arnow reactivity (24). HPLC chromatograms of the resuspended compounds indicate the presence of multiple peaks that absorbed at both 220 and 280 nm (a typical spectrum is presented in Fig. 1). Each peak (P1–P6) was subjected to ESI-TOF MS. Six major catecholic compounds (A, $m/z = 278$; B, $m/z = 351$; C, $m/z = 400$; D, $m/z = 431$; E, $m/z = 473$; F, $m/z = 553$) were detected (chemical structures are described below), but most of the HPLC peaks contained mixtures of these compounds to varying degrees. Two of the HPLC peaks, P3 and P6, however, were homogeneous, as seen from the ESI-TOF MS chromatograms (P3 = A, Fig. 2*b*, and P6 = C, Fig. 2*c*, note that compound A in this chromatogram is also a fragment of C, as explained in the next section), but these compounds were also detected within other HPLC fractions. For instance, P2 contained 5 compounds (A, B, D, E, and F; Fig. 2*a*). In some cases, the peaks contained sodiated ions. The letters on each peak represent the catecholic cross-links subsequently identified by fragmentation. Mass-to-charge (m/z) ratios are presented in Table 1. P3 and P6 were the peaks that were also purified in yields sufficient for ^1H NMR characterization.

To test which strategy *Dosidicus* employs, we attempted extraction of catecholic precursor compounds from the buccal tissues producing the beaks, which were initially screened using the Arnow stain (26). Preliminary results using gel-filtration chromatography and PAGE on extracted buccal tissues confirm that the major catecholic precursor of beak has a low molecular weight and that Arnow reactive substance is mostly not protein-bound (data not shown).

MS/MS—Fragmentation patterns of the major compounds detected by ESI-MS are presented in Fig. 3. It has been established elsewhere (see supplementary on-line materials of Ref. 20) that fragmentation patterns of (m/z) = 278 (Fig. 3*a*) and 351 peaks correspond to (His)-4-methylcatechol (4MC) and His-dopa couplings, respectively, both of which exhibit the $m/z =$

FIGURE 3. MS/MS fragmentation patterns of isolated catecholic compounds. *a*, $m/z = 278$; *b*, $m/z = 400$, which is identical to $m/z = 278$ plus 4MC, *i.e.* the trimer, 4MC-His-4MC; *c*, $m/z = 553$ is consistent with a tetramer His-4MC-His-4MC. Fragmentation of 431 was also acquired (data not shown), and the fragmentation pattern looked identical to that of $m/z = 553$ up to $m/z = 431$, which corresponds to His-4MC-His. Note that both $m/z = 400$ and 431 can be derived from the tetramer $m/z = 553$.

TABLE 2

H NMR peak assignment for cross-links $m/z = 278$ (left) and $m/z = 400$ (right)

$m/z = 278$			$m/z = 400$		
Chemical shift	Coupling constant (doublet)	Assigned protons	Chemical shift	Coupling constant (doublet)	Assigned protons
8.6167		Imidazole, δ_2	8.586		Imidazole, δ_2
7.3299		Imidazole, ϵ_1	7.4023		Imidazole, ϵ_1
6.9154	$J = 9.55$	Ortho-catechol, C5	6.9119		Para-catechol, C5
6.8963		"	6.8958		Para-catechol, C5 (tautomer 2)
6.8424	$J = 8.05$	Ortho-catechol, C6	6.869		Para-catechol, C3
6.8263		"	6.8193	$J = 9.65$	Ortho-catechol, C5
5.1902		Vinylic H, ortho-catechol (tautomer 2)	6.800		"
3.9432		α -histidine	6.7244	$J = 8.2$	Ortho-catechol, C6
3.9302		α -histidine, split by β	6.708		"
3.917		"	5.1879		Vinylic H, ortho-catechol (tautomer 2)
3.2352		β -histidine	5.1545		Vinylic H, para-catechol (tautomer 2)
3.2224		β -histidine, split by α	3.7122		α -histidine
2.177		Methyl (tautomer 1)	3.6987		α -histidine, split by β
			3.6848		"
			3.1936		β -histidine
			3.1792		β -histidine, split by α
			3.1585		"
			3.1449		"
			2.1788		Methyl (tautomer 1)

156 (His + H⁺) ion fragment reported earlier (27). The fragmentation pattern of (m/z) = 400 (Fig. 3b) shows that it is closely related to (m/z) = 278, plus an added mass of 122 Da consistent with the presence of another methylcatechol (or quinone-methide) perhaps bound to the second imidazolic nitrogen. Fragmentation patterns of (m/z) = 431 and 553 also show striking similarities with those of (m/z) = 278 and 400 (Fig. 3c). For (m/z) = 553, there is an initial mass loss of 122 Da, with the resulting ion (m/z) = 431. The additional mass loss of 153 Da can then be attributed to dehydrohistidine, resulting in the cross-link dimer (m/z) = 278. The fragmentation pattern of (m/z) = 431 (not shown here) was identical to that of (m/z) = 553 from (m/z) = 0 to (m/z) = 431. Hence, all of the detected cross-links after hydrolysis can be deconstructed from the initial tetramer (m/z) = 553, which corresponds to His-4MC-His-4MC. Removing one His gives rise to (m/z) = 400, whereas removing a 4MC yields (m/z) = 431. Extra loss of either 4MC or His, respectively, finally results in the initial building block (m/z) = 278 in both cases.

¹H NMR—¹H NMR spectra of the dimeric cross-link compound (His-4MC) purified by C18 HPLC is presented in Fig. 4, and assigned peaks are given in Table 2. The aromatic region of the spectrum (enlarged in Fig. 4b) contains a pair of doublets, with J -coupling constants between 8 and 10. These values are consistent with ortho-pairing of hydrogen groups on the ring. The aromatic region also contains a peak at 7.3 ppm assigned to the δ_2 ring H of imidazole histidine (Creighton system). A peak farther from the aromatic region at 8.62 is attributed to the second hydrogen of the imidazole ring (ϵ_1). The *o*-placement of ring hydrogens hence suggests that the linkage between the catechol and histidine must occur at the sterically encumbered 2-position of the catechol ring. The additional peak at 5.19 ppm cannot be attributed to any hydrogen atom of the His-4MC cross-link. However, its location is in the

region of vinylic hydrogen and is consistent with the coexistence of quinone-methide tautomer with cross-linked (His-4MC) in solution.⁴ In addition, the larger peak height of the vinylic H *versus* that of the methyl H suggests that the equilibrium is shifted toward the quinone-methide tautomer.

The ¹H NMR spectrum for catechol-His-catechol adduct (m/z) = 400 (see Fig. S1), contains a total of seven signals between 6.9119 ppm and 6.7080 ppm, including two doublet peaks, implying that the orthohydrogens of the dimer adduct remain present with J -coupling values of 8. The additional three peaks are not coupled and must correspond to the protons of the second catechol. The absence of coupling indicates that the protons are paraoriented (as opposed to ortho on the first catechol). Had the second catechol contained ortho- or metahydrogens, a second set of coupled doublets would be present in this region of the spectrum. The presence of three peaks (as opposed to two) is again attributed to tautomerization, which slightly affects the local environment and hence yields two distinct peaks. Additionally, the two peaks corresponding to the imidazole ring protons (7.402 and 8.586 ppm) are confirmed. Therefore, one catechol is attached to the histidine via the 2-position of the aromatic ring whereas the other catechol is attached via the 6-position. As in the (m/z) = 278 spectrum, the vinylic hydrogens of the quinone-methides are present, with two distinct peaks (5.1879/5.1545 ppm) and an integration that approximates to four protons, suggesting that both catechols are partially oxidized. The extracted HPLC compound is thus deemed to be a mixture of tautomers with various levels of oxidation of the catecholic/quinone rings. Although all adducts described are present in hydrolysates, their concentration relative to one another is unknown, making it difficult to infer whether there is a prevailing cross-link or whether they all derive from the degradation of the tetrameric cross-link (His-4MC-His-4MC). Our previous work (20), however, did establish that the total cross-link content in the hard rostrum of the beak is as much as 15 weight %, which is an extremely high value compared with any natural or synthetic polymer.

DISCUSSION

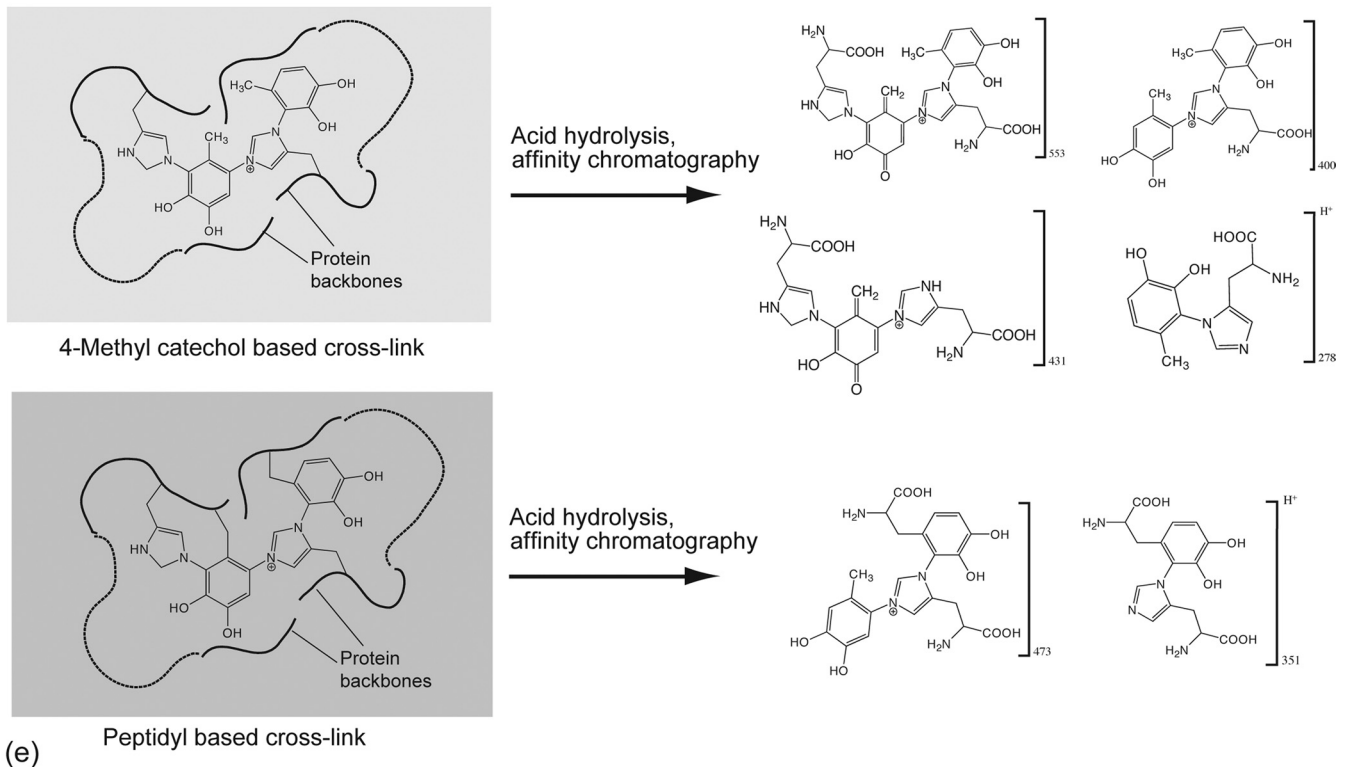
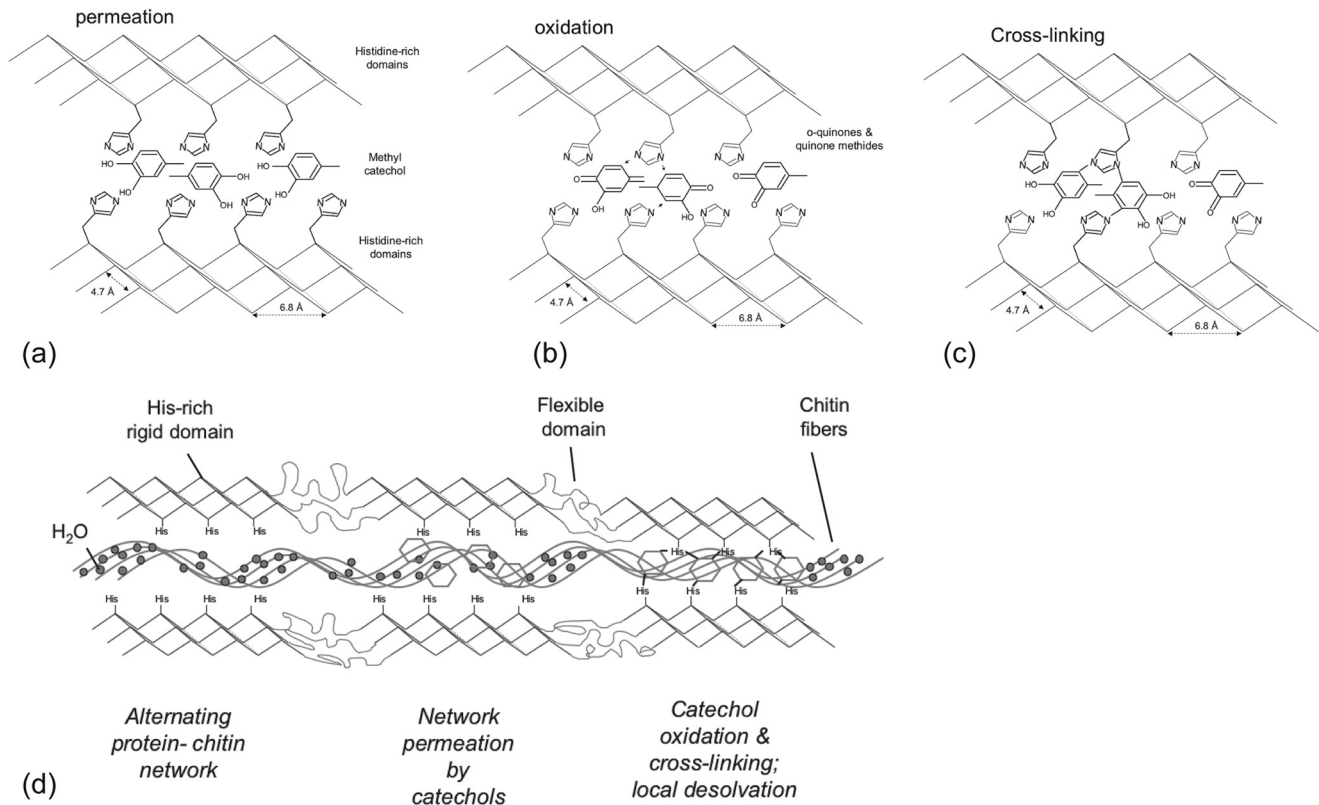
Jumbo squid beaks (and the beaks of other cephalopods such as octopus and cuttlefish) represent an intriguing paradigm of composite materials processing for several reasons. Beaks are produced in a wet environment, grow continuously during the lifespan of the animal (28, 29), and are fabricated with macroscopic biochemical gradients resulting in a wide range of mechanical properties, namely a flexible proximal region attached to the buccal mass and a hard, stiff rostrum at the distal end. Previous investigations established the presence of His-dopa adducts in squid beak and proposed them to be stabilizing cross-links of the composite proteinaceous matrix. The His-4MC detected by MS/MS (m/z) = 278) was assumed to result from the fragmentation-induced cleavage of the bond

⁴ Strictly speaking, the quinone methide is not a tautomer of 4-methyl catechol but of the *o*-quinone, a facile oxidation product of 4MC by the loss of 2 hydrogens. As such, the term "tautomer" is used throughout to emphasize the co-existence of 4MC, quinone-methide and orthoquinone.

between the α and β side chain carbons of dopa in the His-dopa cross-link during ionization in the source region (20). Present results reveal a more complex picture. In addition to the

dimeric His-dopa cross-link, trimeric and tetrameric 4MC-His derivative adducts are released from the beak during hydrolysis. The absence of dopa in any of these multimers

Model of structure and desolvation



Cross-linking Chemistry of Squid Beak

suggests that 4MC arises instead from a low molecular weight precursor.

In insect cuticle, a variety of catecholic agents, such as *N*-acetyldopamine or 3,4-dihydroxyphenylethanol, among others (30, 31) and including their quinone-methide tautomers (32) are known to interact covalently with proteins during sclerotization. Quinone-methide tautomer formation (as detected by both MS/MS and H NMR) could be occurring during post-isolation processing or appears *in situ* as an intermediate cross-linking agent as reported in some cuticles (32). After an initial oxidation step, which converts the catechol to a quinone, the latter is coupled to nucleophilic protein side chains, particularly histidine and cysteine, when present (33). The tendency of His to undergo nucleophilic addition to *o*-quinone was further confirmed in synthetic self-assembling polymers (34) with the additional important insight that cross-linking efficiency was only high when reactive functionalities were brought together by the formation of complementary secondary structures; cross-linking in disordered isotropic solutions was negligible.

Tri- and tetrameric cross-links involving covalent bonding of both nitrogens of the imidazole moiety have not been previously reported. In insect cuticles, the nucleophilic attack of phenolic rings by His residues usually occurs at the 5- and 6-positions (19, 27) whereas the C2 carbon is also targeted in model studies (35). Our data suggest that the C2 carbon is coupled to the His imidazole in the hydrolyzed dimer. Although this seems a sterically less favorable position for a dimeric cross-link, the catecholic ring is also bound to a second His residue through the 6-position in the larger cross-links. It is plausible that the C2 site is detected simply because it is more stable during hydrolysis than the 5- or 6-position, or that *in situ*, the quinone is presented to His residues in such a way that the 2-adduct is favored. Regardless of the details of cleavage during acid hydrolysis, the strategy of using tri- and tetrameric cross-links is unique and is probably related to the high cross-link density in the mature beak (as much as 15% dry weight) (20). The engineered juxtaposition of reactive groups such as quinone and histidine is known to promote cross-linking reactions (34). In insect cuticular proteins, a consensus sequence (“R&R consensus”) involved with chitin binding (11, 36, 37) has been identified: in addition to the ideal location of His residues in the R&R consensus for subsequent cross-linking reactions, the consensus is predicted to form β -pleated sheets (36). Provided that His-rich domains in the beak proteins are also arranged according to a β -sheet conformation, they might play a role of stiff elements with a highly packed configuration, in which His residues are strategically presented by one or both faces of a series of sheets to be joined by reaction with the catecholic cross-linkers, as schematically illustrated in Fig. 5. As cross-linking reactions ensue, water molecules are squeezed out, thereby

leading to chitin desolvation. To test this hypothesis, a full sequence of beak proteins will be necessary, a task that has so far been precluded by the intractability of cross-linked proteins in the tip region.

Bioprocessing of the chitin/water/protein composite shares parallels with the impregnation processes by which many thermoset polymer matrix composites are fabricated. In this scenario, chitin nanofibrils are assumed to form the initial template, similar to glass fibers or carbon fiber mats in composite processing. Protein “fillers” and catechols are then secreted through the chitinous preform. Once oxidation of catechols moieties has been triggered (either by autoxidation or enzymatic processes), cross-linking and hardening (sclerotization) ensue (see Fig. 5*d*). In the chitin/protein biocomposite, however, there is a critical additional variable, water. As sclerotization proceeds, water is indeed progressively expelled from the material. This precise role of water removal on the structural properties of the beak is especially critical and not yet fully understood, in part because the effect of water on the individual components of the composite is poorly understood. The elastic modulus (or Young’s modulus E_c) of fully dried chitin fibers has been reliably measured in only one study (in which cellulose was ascertained as a control), and values ranging from 40 to 65 GPa were reported (38). In the hydrated state, there is considerable variation in moduli reported for chitosan (chitin) scaffolds, but 10–20 MPa effectively represents the range (39–41) (fully hydrated conditions). Hence, a critical observation, regardless of the exact numbers, is that there are at least 3 orders of magnitude difference in the stiffness of chitin/chitosan between the fully hydrated state (where it is present as a porous, water-saturated scaffold) and the dry state. In *Dosidicus* beaks, the modulus in the untanned (mostly chitinous) region is about 50–60 MPa (hydrated conditions) and reaches around 5 GPa in the distal, fully tanned beak, which contains about 15% of residual water. As schematically illustrated in Fig. 6, the effective boundaries are the “pure” chitin fibers in fully hydrated and dried conditions, respectively. What are the implications of this for cross-linking and the graded properties of squid beaks? In an attempt to mimic the action of catechols during sclerotization to stiffen chitosan scaffolds, Wu *et al.* (40) achieved a 2-fold increase in stiffness after treatment with chitosan films with catechols. Although this represents a significant increase in stiffness, it is far below the 100-fold increase observed in *Dosidicus* beaks. Quinone coupling has also been shown to stabilize weak gelatinous protein scaffolds (42). Perhaps the major role of catecholic cross-linking is to remove water irreversibly by creating a hydrophobic biocomposite. Additionally, it may also displace water by using phenolic hydroxyls to outcompete H-bonding by water. Sclerotization triggered by low molecular weight catechols may offer better

FIGURE 5. Proposed mechanisms of sclerotization and desolvation in squid beaks. *a*, in the secondary structure of the sclerotized proteins, it is hypothesized that there are strategically placed His residues for subsequent cross-linking with catecholic moieties, secreted by catecholic glands in the buccal mass that diffuse through the chitinous scaffold. *b*, the catechols are then oxidized into *o*-quinones, which subsequently react with His-rich domains (*c*). *d*, as catechol oxidation and cross-linking occurs, water molecules bound to chitin fibers are simultaneously expelled from the biocomposite, resulting in localized and controlled dehydration, with a high density of covalent cross-links that eventually form the solid macromolecular structure. It is unknown whether the process is oxidase-driven or nonenzymatic. *e*, matrix cross-link derivatives as deduced from hydrolysates are depicted and consist of a family of His-4MC as well as His-dopa dimers, trimers, and tetramers. The relative concentration of adducts shown in *e* is unknown, as well as the physicochemical details of the chitin/matrix interactions (chitin is not shown in the model).

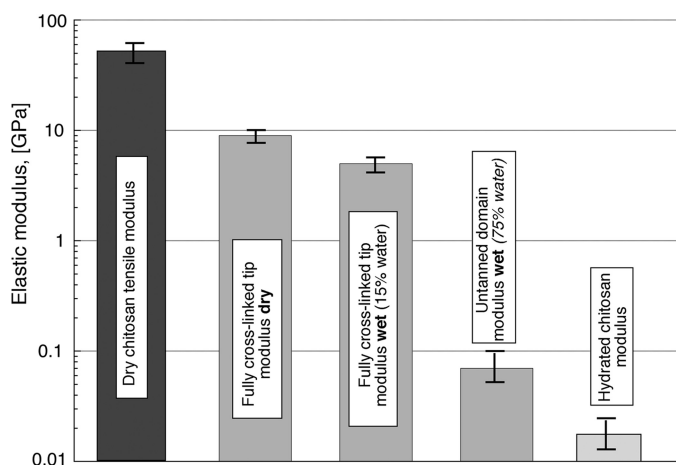


FIGURE 6. Elastic modulus (stiffness) of *D. gigas* beaks and comparison with values for fully dried chitosan nanofibers and hydrated chitosan scaffolds. Note that the stiffness values of the tanned (highly cross-linked) tip and hydrated untanned (nonsclerotized) tip fall between the moduli for dry chitin/chitosan and hydrated chitin/chitosan materials. Data are from Refs. 20, 38–40.

spatial control of cross-linking compared with more stationary peptidyl-bound dopa once thought of as a more primitive model of cross-linking. Sclerotization triggered by low molecular weight catechols may offer better spatial control of cross-linking compared with tethered peptidyl-bound dopa. Moreover, it may be possible to add small catechols to the beak at any time during or after its formation, thereby enabling readjustments to the local levels of cross-linking, dehydration, and stiffening. As in the formation of mussel threads by dopa-containing proteins (43, 44), there is no direct physical interaction between the beak precursors and bulk water. The secretion process occurs in a physically insulated environment between the beak and the muscular buccal mass of the squid and is necessary to prevent the diffusive loss of proteins and catechols.

Covalent cross-linking is undoubtedly important in the stiffening and hardening of beak (45). It is, however, only one of many strategies, both molecular and microstructural, in Nature for tuning the overall mechanical properties of macromolecules. Water access to chitin nanofibers encased by a highly cross-linked supramolecular network saturated with hydrophobic and H-bonding catecholic rings is highly restricted. From a thermodynamic perspective, cross-linking may serve to increase the glass transition temperature of the biocomposite. As in other structural tissues such as silk (46), understanding the complexities of protein solvation may be key to designing chitin/protein composites with physical properties that are tailored on a macroscopic scale.

Although high hardness and stiffness are controlled primarily at the molecular length scale, toughness or resistance to crack propagation (another critical structural characteristic for beak function), is governed at the microstructural length scale. Like virtually all hard biological materials, squid beak exhibits a hierarchical organization known to increase the toughness of biological composite structures well above that of their building blocks (3, 4, 47). The beak has a lamellar organization (48), which deflects propagating cracks, redistributes stresses in front of cracks, and necessitates renucleation of cracks in neigh-

boring lamellae. These are energy-dissipating processes that ultimately endow the beak with a high fracture toughness (48). To truly understand beak performance, insights from further microstructure analysis must be added to the molecular scale models such as that proposed in Fig. 5.

CONCLUSION

Dosidicus beak contains a high density of covalent cross-links that pack its constitutive macromolecules into a tight supramolecular network, resulting in high stiffness, hardness, and intensely dark coloration. These cross-links were isolated from beak after acid hydrolysis and subsequently resolved by affinity chromatography and HPLC. Spectroscopic studies by MS/MS and ^1H NMR reveal that the cross-links represent a family of multimeric catecholic-histidine adducts. Tetrameric cross-links between His residues and catecholic moieties are suggestive of an unusually high cross-link density within the mature material. The most abundant catechol is 4MC, not dopa; indeed, 4MC and dopa may represent separate but converging pathways in the beak. We propose that the beak is produced by a process reminiscent of the manufacture of fiber-reinforced composites whereby chitin fibers form an initial scaffold subsequently impregnated by a blend of proteins and catechols and cured via catecholic cross-linking. Better elucidation of the proteins and catecholic precursors from appropriate secretory glands should provide critical insights into the biosynthetic pathway by which the graded chitin/protein composite is formed, as well as how such an extremely tight cross-link assembly is achieved. Indeed, squid beak is an excellent model system for the bioinspired fabrication of environmentally sustainable load-bearing materials.

Acknowledgments—We thank C. Taylor (Louisiana State University) and A. Srivastava (Indian Institute of Science Education and Research, Bhopal, India) for help with NMR data acquisition and insists about analysis, and J. Pavlovic (Department of Chemistry, University of California Santa Barbara) for help with tandem MS operation.

REFERENCES

1. Uyeno, T. A., and Kier, W. M. (2005) *J. Morphol.* **264**, 211–222
2. Kamat, S., Su, X., Ballarini, R., and Heuer, A. H. (2000) *Nature* **405**, 1036–1040
3. Barthelat, F., Tang, H., Zavattieri, P. D., Li, C.-M., and Espinosa, H. D. (2007) *J. Mech. Phys. Solids* **55**, 306–337
4. Meyers, M. A., Chen, P. Y., Lin, A. Y. M., and Seki, Y. (2008) *Prog. Materials Sci.* **53**, 1–206
5. Weaver, J. C., Wang, Q., Miserez, A., Tantuccio, A., Stromberg, R., Bozhilov, K. N., Maxwell, P., Nay, R., Heier, S. T., Dimasi, E., and Kisailus, D. (2010) *Materials Today* **13**, 42–52
6. Schofield, R. M., Nesson, M. H., Richardson, K. A., and Wyeth, P. (2003) *J. Insect Physiol.* **49**, 31–44
7. Broomell, C. C., Zok, F. W., and Waite, J. H. (2008) *Acta Biomater.* **4**, 2045–2051
8. Khan, R. K., Stoimenov, P. K., Mates, T. E., Waite, J. H., and Stucky, G. D. (2006) *Langmuir* **22**, 8465–8471
9. Birkedal, H., Khan, R. K., Slack, N., Broomell, C., Lichtenegger, H. C., Zok, F., Stucky, G. D., and Waite, J. H. (2006) *ChemBioChem* **7**, 1392–1399
10. Vincent, J. F. V. (2002) *Composites Part A: Appl. Sci. Manufacturing* **33**, 1311–1315

Cross-linking Chemistry of Squid Beak

11. Iconomidou, V. A., Willis, J. H., and Hamodrakas, S. J. (2005) *Insect Biochem.* **35**, 533–560
12. Andersen, S. A. (1981) *J. Insect Physiol.* **27**, 393–396
13. Vincent, J. F. V., and Ablett, S. (1987) *J. Insect Physiol.* **33**, 973–979
14. Vincent, J. (2001) in *Encyclopedia of Materials Science and Technology* (Buschow, K. H., Flemings, M. C., Kramer, E. J., Cahn, R. W., Ilschner, B., and Mahajan, S., eds) pp. 1924–1928, Elsevier, New York
15. Andersen, S. A. (2010) *Insect Biochem.* **40**, 166–178
16. Pryor, M. G. M. (1940) *Proc. R. Soc. Lond. B Biol. Sci.* **128**, 393–407
17. Pryor, M. G. M. (1962) in *Comparative Biochemistry* (Florin, M., and Mason, H. S., eds), pp. 371–396, Academic Press, New York
18. Andersen, S. A. (1985) in *Comprehensive Insect Physiology Biochemistry and Pharmacology* (Kerkut, G. A., and Gilbert, L. I., eds) pp. 59–74, Pergamon Press, New York
19. Kramer, E. J., Kanost, M. R., Hopkins, T. L., Jiang, H., Zhu, Y. C., Xu, R., Kerwin, J. L., and Turecek, F. (2001) *Tetrahedron* **57**, 385–392
20. Miserez, A., Schneberk, T., Sun, C., Zok, F. W., and Waite, J. H. (2008) *Science* **319**, 1816–1819
21. Barnes, H. H., and Ishimaru, C. A. (1999) *BioMetals* **12**, 83–87
22. Zhao, H., Sun, C., Stewart, R. J., and Waite, J. H. (2005) *J. Biol. Chem.* **280**, 42938–42944
23. Zhao, H., and Waite, J. H. (2005) *Biochemistry* **44**, 15915–15923
24. Waite, J. H., and Tanzer, M. L. (1981) *Anal. Biochem.* **111**, 131–136
25. Fetterer, R. H., and Hill, D. E. (1994) *J. Parasitol.* **80**, 952–959
26. Rubin, D., Miserez, A., and Waite, J. H. (2010) in *Advances in Insect Physiology* (Casas, J., ed) pp. 75–133, Elsevier, New York
27. Kerwin, J. L., Turecek, F., Xu, R., Kramer, K. J., Hopkins, T. L., Gatlin, C. L., and Yates, J. R., 3rd (1999) *Anal. Biochem.* **268**, 229–237
28. Kear, A. J. (1994) *J. Mar. Biol. Assoc. U.K.* **74**, 801–822
29. Hernandez-Garcia, V. (2003) in *Coleoid Cephalopods through Time*, Proceedings of Conference, Berlin, Germany (Warnke, K., Jeupp, H., and Boletzky, S. V., eds) Berliner Paläobiologie Abhandlung, Berlin, Germany
30. Sugumaran, M. (1991) in *Physiology of the Insect Epidermis* (Binnington, K., and Retnakaran, A., eds) pp. 141–168, CSIRO Publications, Melbourne, Australia
31. Hopkins, T. L., and Kramer, K. J. (1991) in *Physiology of the Insect Epidermis* (Binnington K., and Retnakaran, A., eds) pp. 213–239, CSIRO Publications, Melbourne, Australia
32. Sugumaran, M., Semensi, V., Kalyanaraman, B., Bruce, J. M., and Land, E. J. (1992) *J. Biol. Chem.* **267**, 10355–10361
33. Schaefer, J., Kramer, K. J., Garbow, J. R., Jacob, G. S., Stejskal, E. O., Hopkins, T. L., and Speirs, R. D. (1987) *Science* **235**, 1200–1204
34. Liu, B., Burdine, L., and Kodadek, T. (2006) *J. Am. Chem. Soc.* **128**, 15228–15235
35. Xu, R., Huang, X., Morgan, T. D., Prakash, O., Kramer, K. J., and Hawley, M. D. (1996) *Arch. Biochem. Biophys.* **329**, 56–64
36. Hamodrakas, S. J., Willis, J. H., and Iconomidou, V. A. (2002) *Insect Biochem.* **32**, 1577–1583
37. Rebers, J. E., and Willis, J. H. (2001) *Insect Biochem.* **31**, 1083–1093
38. Nishino, T., Matsui, R., and Nakame, K. (1999) *J. Polym. Sci. Part B Polym. Phys.* **37**, 1191–1196
39. Madhally, S. V., and Matthew, H. W. (1999) *Biomaterials* **20**, 511–521
40. Wu, L. Q., Ghodssi, R., Elabd, Y. A., and Payne, G. F. (2005) *Adv. Funct. Materials* **15**, 189–195
41. Wu, L. Q., McDermot, M. K., Zhu, C., Ghodssi, R., and Payne, G. F. (2006) *Adv. Funct. Materials* **16**, 1967–1974
42. Yamauchi, A., Hatanaka, Y., Muro, T., and Kobayashi, O. (2009) *Macromol. Biosci.* **9**, 875–883
43. Waite, J. H. (2002) *Integr. Comp. Biol.* **42**, 1172–1180
44. Waite, J. H., Holten-Andersen, N., Jewhurst, S. A., and Sun, C. (2005) *J. Adhesion* **81**, 297–317
45. Vincent, J. F., and Wegst, U. G. (2004) *Arthropod Struct. Dev.* **33**, 187–199
46. Porter, D., and Vollrath, F. (2009) *Adv. Materials* **21**, 487–492
47. Paris, O., Burgert, I., and Fratzl, P. (2010) *MRS Bull.* **35**, 219–225
48. Miserez, A., Li, Y., Waite, J. H., and Zok, F. (2007) *Acta Biomater.* **3**, 139–149